

Ejection-Collision orbits in the symmetric collinear four-body problem

M. Alvarez-Ramírez

Dept. de Matemáticas, UAM–Iztapalapa, 09340 Iztapalapa, Ciudad de México, México

E. Barrabés

Dept. Informàtica Matemàtica Aplicada i Estadística, Universitat de Girona, Girona, Spain

M. Medina

Dept. de Matemáticas, UAM–Iztapalapa, 09340 Iztapalapa, Ciudad de México, México

M. Ollé

*Dept. Matemàtiques Universitat Politècnica de Catalunya,
Av Diagonal 647, Barcelona 08028, Spain*

Abstract

In this paper, we consider the collinear symmetric four-body problem, where four masses $m_3 = \alpha$, $m_1 = 1$, $m_2 = 1$, and $m_4 = \alpha$, $\alpha > 0$, are aligned in this order and move symmetrically about their center of mass. We introduce regularized variables to deal with binary collisions as well as McGehee coordinates to study the quadruple collision manifold for a negative value of the energy. The paper is mainly focused on orbits that eject from (or collide to) quadruple collision. The problem has two hyperbolic equilibrium points, located in the quadruple collision manifold. We use high order parametrizations of their stable/unstable manifolds to devise a numerical procedure to compute ejection-collision orbits, for any value of α . Some results from the explorations done for $\alpha = 1$ are presented. Furthermore, we prove the existence of ejection-direct escape orbits, which perform a unique type of binary collisions.

Keywords: collinear four-body problem, ejection/collision orbits, binary

Email addresses: `mar@xanum.uam.mx` (M. Alvarez-Ramírez), `esther.barrabes@udg.edu` (E. Barrabés), `mvmg@xanum.uam.mx` (M. Medina), `Merce.Olle@upc.edu` (M. Ollé)

1. Introduction

The classical n -body problem studies the dynamics of n point masses interacting according to Newtonian gravity. In the symmetric collinear four-body problem, the bodies are symmetrically distributed about the centre of mass by
5 pairs, each of those pairs have equal mass and the configuration of the four bodies is collinear at every instant. It is a two degrees of freedom problem which is a sub-problem of the trapezoidal four-body problem that has three degrees of freedom, see the works of Lacomba and Simó ([1, 2]).

The four-body problem has attracted the attention of numerous astronomers
10 since through it, the gravitational interaction of many stellar or exoplanetary systems can be modelled, as the interaction of two binary star systems or the interplay of two planets with a binary star system. Many of the studies, as the influence between two binaries, have been carried out from the numerical point of view ([3], [4], [5], [6]). Also, the close interaction of systems of few stars give
15 rise to the possibility of collisions between two or more stars in a cluster, as close encounters and direct physical collisions between stars are frequent in globular clusters, [7]. These collisions are more frequent as a binary-binary system than as a system formed by a single star and a binary one. Other numerical studies have been conducted to understand the numerical scattering of the influence
20 between binary-binary or single-binary systems, see [8].

We focus on the particular case of the collinear model of a four body problem. A solution of the symmetric collinear four-body problem, denoted by SC4BP, experiences a collision if two or more particles come together at a certain time. At such a time the potential energy approaches infinity, the equations of motion
25 become undefined and the solution has a singularity. The analytical and numerical study of this problem requires the McGehee's blow up technique to regularize the singularity corresponding to total (quadruple) collision and the

regularization of binary collisions –i. e. collisions between m_1 and m_2 – and simultaneous binary collisions –i. e. m_1 and m_3 collide as well as m_2 and m_4 –
30 (see for example [9] and [10]). This singularity due to total collision is blown up and in its place is glued an invariant total collision manifold. Simó and Lacomba [2] analysed the flow on the total collision manifold and they found a family of connection orbits between two quadruple collisions which arise as the parameter of masses is varied. The flow on this manifold provides relevant information for
35 the flow close to quadruple collision.

In addition to the mentioned works of Simó and Lacomba, several papers can be found in the literature on the symmetric collinear four-body problem. Sweatman, [11] in the particular case of equal masses for the four bodies, finds very interesting dynamical phenomena for the problem under study, showing
40 the existence of periodic, quasiperiodic, fast-scattering and chaotic-scattering orbits. Still in the case of equal masses, Sekiguchi and Tanikawa [12] study the SC4BP both analytically and numerically. In particular, they classify a great variety of orbits by means of symbol sequences and they obtain the initial conditions leading to escape using escape criteria established in the paper.

45 Focussing on periodic orbits, Ouyang and Yan [13] and Huang [14] analytically prove the existence of Schubart-like periodic orbits by applying variational calculus. Schubart-like orbits are periodic solutions with exactly two binary collisions and one simultaneous binary collision per period. Later on, Bakker et al. [15] and Sweatman [16] analyse their stability depending on the mass
50 parameter.

We finally mention, for the symmetric collinear four-body problem, the papers by Alvarez et al. [9, 17], where the authors provide some analytical results concerning singularities and regularization, and analytically study the quadruple collision manifold, the equilibrium points, the infinity manifold and the
55 relation between both manifolds which allow them to prove the existence of orbits connecting quadruple collision and infinity. For the collinear non symmetric four-body problem, in [18], Mather and McGehee prove the existence of solutions which become unbounded in finite time for special values of the

masses.

60 The main goal in this paper is to amalgamate both theoretical and numerical tools to investigate, on one hand, orbits that eject from quadruple collision and have a fast escape to infinity, and, on the other hand, ejection-collision orbits (also denoted by ECO), that is orbits that eject from quadruple collisions and go back to quadruple collision. The latter are regarded as heteroclinic connections
65 between the two equilibrium points (that lie on the total collision manifold). In order to numerically compute ejection-escape orbits and ejection-collision ones we need the construction of parametrizations, up to certain order, of the stable and unstable invariant manifolds, W^s and W^u , of the equilibrium points, using the methodology explained in [19]. At this point we mention the work of
70 Sekiguchi and Tanikawa, [12], where, due to the Poincaré section considered, the ejection-collision orbits are all mixed up and undistinguishable. In the present paper a different Poincaré section has been taken into account that allows to classify and distinguish different types of ejection-collision orbits. Following this classification, Lacombe and Medina in [20] proved analytically the existence of
75 certain ejection collision orbits for specific values of the mass parameter. In this paper, a numerical method is explained to compute ECO for any value of the mass parameter α and negative energy h . The results are presented for $\alpha = 1$ and $h = -1$.

The paper is organized as follows: in Section 2, we recall briefly some
80 known results about the dynamics of the SC4BP, including the regularization of total collision using McGehee's coordinates [10], the regularization of binary collisions, the description of the flow on the quadruple collision manifold and the existence of two hyperbolic equilibrium points, E^\pm . We compute high order parametrizations of the associated stable and unstable invariant manifolds,
85 $W^{s,u}(E^\pm)$ and some error tests have been carried out to control the accuracy of the approximations. Section 3 is devoted to the orbits that eject from (or collide to) quadruple collision and directly escape to (come from) infinity describing a unique type of binary collisions. In Section 4 we present some properties of the ejection-collision orbits and devise a numerical method to compute them. We

90 show the results for the case $\alpha = 1$.

2. The symmetric collinear four body-problem

The aim of this section is to present a summary of the equations and the main properties of the symmetric collinear four-body problem, SC4BP. For more details see, for example, [17, 2] and the references therein. In particular, we focus
 95 on the main features for the computation of ejection/collision orbits (orbits that start/end at a quadruple collision) and ejection-collision orbits (ECO, orbits that start and end at a quadruple collision): the dynamics on the total collision manifold, the stable and unstable invariant manifolds of the equilibrium points and the Poincaré section used.

100 2.1. Equations of the SC4BP

The symmetric collinear four-body problem consists of four point masses, with masses m_i , $i = 1, \dots, 4$, moving on a straight line under the Newton's law of gravitation with $m_1 = m_2$ and $m_3 = m_4$ in symmetric positions with respect to the center of mass at the origin. Without loss of generality, we can suppose
 105 that the first two bodies have mass $m_1 = m_2 = 1$ and are located at $\pm x$, and the other two bodies have mass $m_3 = m_4 = \alpha$, where $\alpha \in (0, \infty)$, and are located at $\pm y/\sqrt{\alpha}$. See Figure 1.

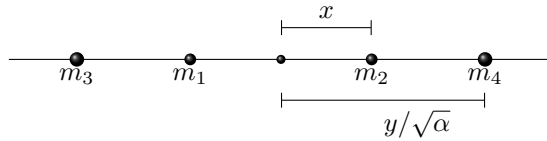


Figure 1: Symmetric collinear four-body problem.

In this set of coordinates, the Hamiltonian of the problem is given by

$$H(x, y, p_x, p_y) = \frac{p_x^2}{4} + \frac{p_y^2}{4} - U(x, y), \quad (1)$$

where $p_x = 2 \frac{dx}{dt}$, $p_y = 2 \frac{dy}{dt}$ and the potential function is

$$U(x, y) = \frac{1}{2x} + \frac{\alpha^{5/2}}{2y} + \frac{2\alpha^{3/2}}{y - \sqrt{\alpha}x} + \frac{2\alpha^{3/2}}{y + \sqrt{\alpha}x}. \quad (2)$$

The phase space of the problem is $\mathcal{U} \times \mathbb{R}^2$ where $\mathcal{U} = \{(x, y) \in \mathbb{R}^2 \mid 0 < \sqrt{\alpha}x < y\}$.

Notice that the equations have three singularities, one at $x = y = 0$, another
 110 at $x = 0$ with $y \neq 0$, and the third one corresponds to $y = \sqrt{\alpha}x \neq 0$. They
 correspond to the following collision configurations:

- **Single binary collision:** the bodies m_1 and m_2 collide, while the other two bodies remain bounded away from them. This type of collision corresponds to $x = 0$ and $y \neq 0$ (collision of type 1 or SBC).
- 115 • **Double (simultaneous) binary collision:** the bodies m_1 and m_3 collide, and by the symmetry of the problem, so do the other two bodies. This double collision corresponds to $y = \sqrt{\alpha}x \neq 0$ (collision of type 2 or DBC).
- **Quadruple collision:** the four bodies collide. This collision corresponds
 120 to $x = y = 0$.

We fix a value of the energy in $H = h$, so the motion takes place in a 3-dimensional manifold and, using (1), it is confined in the configuration space (x, y) to the Hill's region given by

$$\mathcal{R}_h = \{(x, y) \in \mathcal{U} \mid U(x, y) \geq -h\}. \quad (3)$$

The function $U(x, y)$ (given in (2)) is strictly positive for all $(x, y) \in \mathcal{U}$, so for $h \geq 0$ the Hill's region coincides with the configuration space \mathcal{U} , whereas for $h < 0$ the Hill's region is limited by $U(x, y) = -h$. In Figure 2 we show the Hill's region for a negative value of the energy h , and an orbit which ends
 125 at the quadruple collision and performs different binary collisions. We will use the representation of the orbits in the configuration space (x, y) inside the Hill's region \mathcal{R}_h through the paper.

In an N -body problem, bounded motions can only occur if $h < 0$ (see, for example Chapter 4 in [21]). Therefore, to study the ejection-collision orbits we
 130 consider only negative values of the energy.

Furthermore, in order to study the dynamics close to the quadruple collision, it is necessary to describe the total collision manifold and the flow on

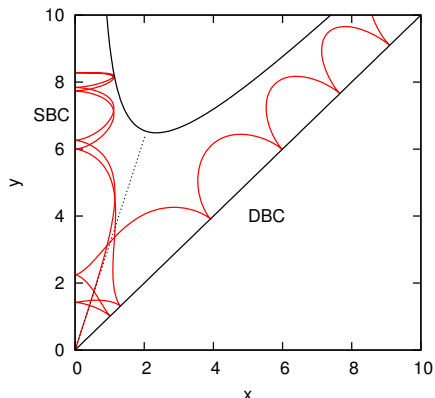


Figure 2: Zero velocity curve and Hill's region (defined in (3)) in the configuration space (x, y) , the homothetic solution (with $\theta = \theta_c$, dotted line, see Section 2.2), and a solution of the SC4BP with single binary collisions (SBC, at $x = 0$) and double binary collisions (DBC, at $y = \sqrt{\alpha}x$) for $\alpha = 1$ and $h = -1$.

it. For this purpose, we apply the blow-up technique introduced by McGehee [10]. Moreover, since the solutions of the SC4BP typically perform several binary collisions, we will also regularize the singularities (due to collisions) that appear in the system of the ordinary of differential equations (ODE). The suitable transformations of the blow up and the regularization in the symmetric collinear four-body problem have been made by Alvarez-Ramírez et. al. [17]. For completeness of the present work, and in order to understand the meaning of the regularized variables, we summarize the changes carried out.

- Introduce polar coordinates

$$\begin{aligned} x &= \frac{r}{\sqrt{2}} \cos \theta, & y &= \frac{r}{\sqrt{2}} \sin \theta, \\ p_x &= \sqrt{2}p_r \cos \theta - \sqrt{2}p_\theta \sin \theta, & p_y &= \sqrt{2}p_r \sin \theta + \frac{\sqrt{2}}{r}p_\theta \cos \theta, \end{aligned}$$

$\theta \in (\theta_\alpha, \frac{\pi}{2})$, where $\theta_\alpha = \arctan(\sqrt{\alpha})$ corresponds to double binary collisions (DBC). The associated potential function is

$$V(\theta) = rU(x, y) = \frac{1}{\sqrt{2} \cos \theta} + \frac{\alpha^{5/2}}{\sqrt{2} \sin \theta} + \frac{2\sqrt{2}\alpha^{3/2}}{\sin \theta - \sqrt{\alpha} \cos \theta} + \frac{2\sqrt{2}\alpha^{3/2}}{\sin \theta + \sqrt{\alpha} \cos \theta}. \quad (4)$$

- Introduce the McGehee's coordinates (v, u) and a change in time through the relations

$$p_r = r^{-1/2}v, \quad p_\theta = r^{1/2}u, \quad dt = r^{3/2}d\tau.$$

- Remove simultaneously all binary collisions, considering the regularized potential

$$W(\theta) = V(\theta) \cos \theta (\sin \theta - \sqrt{\alpha} \cos \theta),$$

which is a positive, real analytic function in $[\theta_\alpha, \pi/2]$, and the change of time and coordinates given by

$$\frac{d\tau}{ds} = \Delta(\theta) = \frac{\cos \theta (\sin \theta - \sqrt{\alpha} \cos \theta)}{\sqrt{W(\theta)}}, \quad w = \Delta(\theta) u. \quad (5)$$

In coordinates (r, v, θ, w) and s as time variable, the equations of the SC4BP become

$$\begin{aligned} \frac{dr}{ds} &= rv\Delta(\theta), \\ \frac{dv}{ds} &= \sqrt{W(\theta)} + \left(2rh - \frac{v^2}{2}\right) \Delta(\theta), \\ \frac{d\theta}{ds} &= w, \\ \frac{dw}{ds} &= -\frac{vw}{2} \Delta(\theta) + (\cos 2\theta + \sqrt{\alpha} \sin 2\theta) \left(\frac{2rh - v^2}{\sqrt{W(\theta)}} \Delta(\theta) + 1\right) \\ &\quad + \frac{W'(\theta)}{W(\theta)} \left(\cos \theta (\sin \theta - \sqrt{\alpha} \cos \theta) - \frac{w^2}{2}\right), \end{aligned} \quad (6)$$

where $W' = \frac{dW}{d\theta}$. The energy relation $H = h$ from (1) becomes

$$w^2 = (2rh - v^2) \Delta(\theta)^2 + 2 \cos \theta (\sin \theta - \sqrt{\alpha} \cos \theta). \quad (7)$$

The vector field defined by equations (6) is an analytic vector field on the phase space $\mathcal{F} = [0, \infty) \times \mathbb{R} \times [\theta_\alpha, \pi/2] \times \mathbb{R}$. The solutions of the ODE, also called *orbits*, will be denoted by $\Gamma = \{\gamma(s)\}_{s \in \mathbb{R}}$ or simply by $\gamma(s)$.

A straightforward computation shows that the set of equations (6) satisfies the symmetry

$$\mathcal{L}_1 : \quad (r, v, \theta, w, s) \rightarrow (r, -v, \theta, -w, -s). \quad (8)$$

Therefore, if Γ is a solution given by $\gamma(s) = (r(s), v(s), \theta(s), w(s))$, then $\bar{\Gamma}$ defined as

$$\bar{\gamma}(s) = (r(-s), -v(-s), \theta(-s), -w(-s)) \quad (9)$$

is also a solution.

Notice that the solutions $\gamma(s)$ and $\bar{\gamma}(s)$ trace the same path in (r, θ) (or (x, y)) coordinates. The paths are traveled in reverse senses. As a consequence, if a solution goes through a point where $v = w = 0$ at a certain time s_0 , then $r(s_0 + s) = r(s_0 - s)$ and $\theta(s_0 + s) = \theta(s_0 - s)$ for all time s . That is, the orbit goes through the same path in configuration space before and after s_0 .

Definition 1. Γ is a symmetric solution (orbit) of equations (6) if there exists an $s_0 \in \mathbb{R}$ such that the curve $q(s) = (r(s), \theta(s))$ satisfies that $q(s_0 + s) = q(s_0 - s)$, $\forall s \in \mathbb{R}$.

Recall that, from (7) and the definition of w (5), $v = w = 0$ means a binary collision (single or double) or a point on the zero velocity curve.

2.2. Total collision manifold, equilibrium points and invariant manifolds

Notice that the system (6) is well defined for $r = 0$, which corresponds to the total collision manifold \mathcal{C} , given by

$$\mathcal{C} = \{(r, v, \theta, w); r = 0, \quad w^2 = -\Delta(\theta)^2 v^2 + 2 \cos \theta (\sin \theta - \sqrt{\alpha} \cos \theta)\},$$

which is a 2-dimensional manifold, topologically equivalent to an sphere minus four points, independent of the total energy h and invariant under the flow (6). The total collision manifold \mathcal{C} belongs to the boundary of the manifold defined by a constant energy, h , for any value of h . Furthermore, the flow on \mathcal{C} is gradient-like with respect the variable v , that is, $dv/ds \geq 0$. See, for more details, [17, 22, 2].

The SC4BP has two equilibrium points

$$E^\pm = (0, \pm v_c, \theta_c, 0) \quad (10)$$

where θ_c is the only solution of $V'(\theta) = 0$ (the potential V is defined in (4)). Furthermore, the SC4BP has a specific solution for which $\theta = \theta_c$ for all $s \in \mathbb{R}$. It is called the *homothetic* solution because the ratio $y/x = \tan \theta_c$ remains constant (see [17]). It is seen as a segment in the configuration plane \mathcal{U} and divides it into two regions: the *region of the DBC* for $\theta \in [\theta_\alpha, \theta_c)$, and the *region of the SBC* for $\theta \in (\theta_c, \pi/2]$. See Figure 2.

Both equilibrium points are hyperbolic: the differential of the vector field evaluated at the equilibrium points has four different real eigenvalues, two positive and two negative, for any value of α , see Lemma 1 in the Appendix. Also, we give explicit formulas for the eigenvalues and the corresponding eigenvectors in terms of α , θ_c and the energy h .

Therefore, there exist the corresponding stable and unstable invariant manifolds $W^s(E^\pm)$ and $W^u(E^\pm)$. On the constant energy manifold their dimensions are the following:

$$\dim(W^u(E^+)) = \dim(W^s(E^-)) = 2, \quad \dim(W^u(E^-)) = \dim(W^s(E^+)) = 1.$$

In particular, the invariant manifolds $W^u(E^-)$ and $W^s(E^+)$ are embedded in the total collision manifold \mathcal{C} . In Figure 3, we plot their projection in the (θ, v) plane for two values of the mass parameter α .

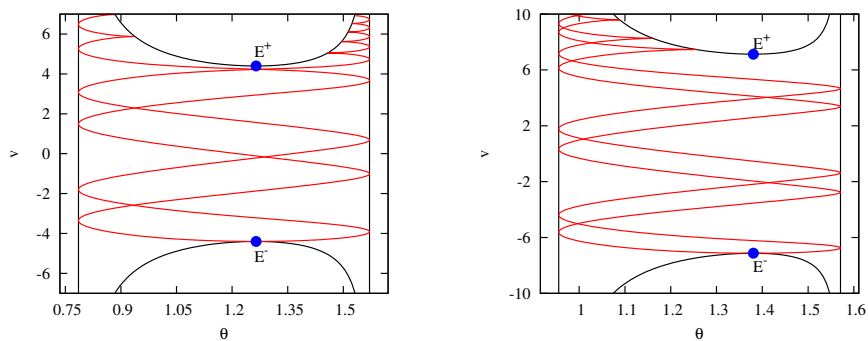


Figure 3: Projection on the (θ, v) plane of the total collision manifold \mathcal{C} and the two branches of the invariant manifold $W^u(E^-)$ for $\alpha = 1$ (left) and $\alpha = 2$ (right). $W^s(E^+)$ can be obtained using the symmetric solution (9).

180 The dynamics on the total collision manifold \mathcal{C} is the key to understand
 the solutions of the SC4BP that go close to quadruple collision, in particular,
 the ejection-collision orbits. In [2], Simó and Lacomba show that there exists
 a sequence of values $\{\alpha_k\}_{k \geq 1}$ for which one or both branches of $W^u(E^-)$ and
 $W^s(E^+)$ coincide (a single or double heteroclinic connection). For values of
 185 $\alpha \in (\alpha_k, \alpha_{k+1})$ the branches of these invariant manifolds (that are contained in
 \mathcal{C}), behave similarly in a topological sense: first they have a number of alternat-
 ing double collisions of both types, and then only perform one type of binary
 collisions as v increases. The number and type of binary collisions of each branch
 of $W^u(E^-)$ (similarly for $W^s(E^+)$) are the same for any $\alpha \in (\alpha_k, \alpha_{k+1})$. In Fig-
 190 ure 3 we show one example where each branch of $W^u(E^-)$ performs different
 type of binary collisions as v increases (left, case $\alpha = 1 \in (\alpha_3, \alpha_4)$) and another
 example where both branches perform the same type of binary collisions (right,
 case $\alpha = 2 \in (\alpha_4, \alpha_5)$). That behavior has been used by Lacomba and Medina in
 [20] to prove the existence of some ejection-collision orbits for specific intervals
 195 of values of α depending on the behavior of the invariant manifold $W^u(E^-)$.

Our purpose in this paper is to give a numerical general methodology that al-
 lows to compute the ejection-collision orbits for any value of α . Clearly, these or-
 bits belong to the intersection of the invariant manifolds $W^u(E^+)$ and $W^s(E^-)$
 in \mathbb{R}^4 . So in order to deal with them, we construct an approximation of their
 parametrizations. The approximations of order one are given by

$$\begin{aligned}
 \Psi_1^-(\xi, \varphi) &= E^- + \xi (\cos(2\pi\varphi) \bar{\sigma}_1 + \sin(2\pi\varphi) \bar{\sigma}_4), \\
 \Psi_1^+(\xi, \varphi) &= E^+ + \xi (\cos(2\pi\varphi) \bar{\sigma}_1 + \sin(2\pi\varphi) \bar{\sigma}_3)
 \end{aligned}
 \tag{11}$$

where $\bar{\sigma}_i$ are the corresponding eigenvectors and $\xi > 0$ is a small fixed quantity,
 the distance from the initial conditions to the equilibrium point. See the Ap-
 pendix for more details and (21) for the specific expressions of the first order
 approximation for each variable. In fact, using the symmetry (9), for any orbit
 200 $\Gamma \subset W^s(E^-)$, we have that $\bar{\Gamma} \subset W^u(E^+)$, and the other way around. Therefore,
 it is enough to construct the parametrization of one of the invariant manifolds.

From the particular expressions for the variables r and θ (see (21) in the

Appendix) we make two remarks. On one hand, we have that $r > 0$ only for values $\varphi \in (1/4, 3/4)$, so these will be the only values considered. The values $\varphi = 1/4, 3/4$ give the parametrization of the orbits of the invariant manifold inside the collision manifold \mathcal{C} . On the other hand, the values $\varphi \in (1/4, 1/2)$ are such that the initial θ satisfies $\theta > \theta_c$, so the orbits start in the region of the SBC, whereas values $\varphi \in (1/2, 3/4)$ correspond to initial values $\theta < \theta_c$, so the orbits start in the region of the DBC. The homothetic solution is obtained when $\varphi = 1/2$.

The vectors $\bar{\sigma}_1$ and $\bar{\sigma}_{3,4}$ give the slow and fast directions, respectively, of the linear dynamics on $W^u(E^+)$, $W^s(E^-)$, so the slow and fast submanifolds are given by $\varphi = 1/2$ and $\varphi = 1/4, 3/4$. The orbits close to the slow direction, which here coincides with the homothetic solution, will be difficult to follow due to the stronger pull of the fast direction. In practice this means that in order to consider orbits close to the homothetic solution, we need to take values $\varphi \in (1/2 - \varepsilon, 1/2 + \varepsilon)$, for ε small enough. As we will show, the richness of the dynamics on the invariant manifold (in the sense of greater variety of orbits exhibiting different number of binary collisions, and in particular to obtain ejection-collision orbits) occurs precisely around the homothetic solution. For example, taking $\alpha = 1$ and $h = -1$, for most of the values $\varphi \in (1/4, 3/4)$, the orbits escape to infinity directly exhibiting only one type of binary collisions (see Section 3), so they are useless in order to compute ejection-collision orbits. If we take the approximation of order one, $\Psi_1^\pm(\xi, \varphi)$, to work with a good precision, for example of order 10^{-12} (see below for details), it will be necessary to consider values of ξ less than 10^{-6} . But, with such small values of ξ , in order to show the richness of the dynamics around the homothetic we need to consider values $\varepsilon \simeq 10^{-9}$.

Therefore, if we want to consider initial conditions close to the slow direction, we need to start farther away from the equilibrium point, that is, with bigger values of ξ . Following [19] (specifically, Chapters 1 and 2), we derive the parametrization of the invariant manifold up to different orders Ψ_m^+ , for $m \leq 8$, and we have performed several numerical tests to control the quality

of the approximation. Following [19] (specifically, Chapters 1 and 2), we derive the parametrization of the invariant manifold Ψ_m^+ , up to different orders $m = 1, 2, \dots$. Then, several numerical tests can be performed to control the quality of the approximation. Specifically, one can compute how big ξ can be in order to maintain a certain accuracy. To do that, for each order m and distance ξ , compute the error in the orbit $e_o(s, \xi, \varphi)$ (see Section 2.5 of [19]) for $s \in [0, 1]$ and the maximum value over all the orbits

$$E_o(\xi) = \max_{\varphi \in (1/4, 3/4)} e_o(1, \xi, \varphi).$$

230 The same procedure can be applied to the errors in the invariance equation and the errors in the energy (see [19] for details). For $\alpha = 1$ and $h = -1$ we have computed $E_o(\xi)$ and the parametrizations Ψ_m^+ for $m = 2, 3, 5, 8$, see Figure 4. For example, in order to have an accuracy below 10^{-8} with $m = 5$ we need ξ up to 0.015 approximately, whereas with $m = 8$ we can take values up to order 0.05.

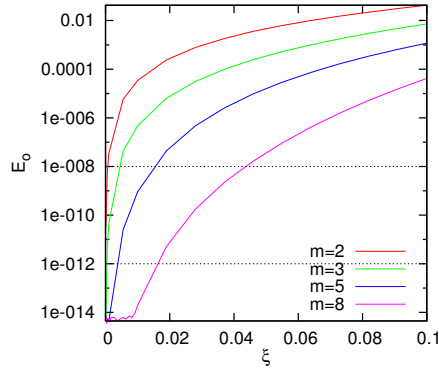


Figure 4: Error of the approximations of the parametrizations Ψ_m for $m = 2, 3, 5, 8$ with respect the distance ξ at which the initial conditions on $W^u(E^+)$ are taken, for $\alpha = 1$ and $h = -1$.

235 For the purposes of this work, we have considered, for $\alpha = 1$, a parametrization of order $m = 8$ and ξ of order 10^{-2} . With these values, we will show that all the ejection-collision trajectories will be found for $\varphi \in (1/2 - \varepsilon, 1/2 + \varepsilon)$, for ε of order 10^{-4} .

2.3. Poincaré section

240 A common tool, in order to study the dynamics of a problem given by
an autonomous system of differential equations, is the Poincaré map, which is
defined on a surface of section. Sekiguchi and Tanikawa, in [12], perform a
wide exploration of the dynamics of the problem using as a surface of section
 $\{\theta = \theta_c\}$. In fact, an orbit cannot cross the section $\{\theta = \theta_c\}$ between two
245 consecutive binary collisions of the same type (see Theorem 7 in [12]).

At this point we want to stress the attention on two important facts for
the computation of ejection-collision orbits. These orbits start and end at $r =$
0, which corresponds to the boundary of the section $\{\theta = \theta_c\}$ in the (v, w)
plane, used by Sekiguchi and Tanikawa [12]. In their representations of the
250 return map to that section, different ejection-collision orbits, that are on that
boundary, share common points. Therefore, they are indistinguishable in that
representation. Moreover, the authors assure in Theorem 1 that all the solutions
of the SC4BP must cross the section $\{\theta = \theta_c\}$ forwards or backwards in time at
least once. That is not true. In the proof the authors forget about the invariant
255 manifolds $W^u(E^+)$ and $W^s(E^-)$. We will show in Section 3 that there exist
orbits that start at a quadruple collision and escape directly without crossing
 $\{\theta = \theta_c\}$ (see Theorem 1) and in Section 4 we will show ejection-collision orbits
that do not cross that section (by cross we always mean transversal intersection).

Taking into account that, typically, all the orbits perform double collisions
(with the exception of the homothetic orbit), we consider the section

$$\Sigma_c = \{(r, v, \theta, w); w = 0, \theta = \theta_\alpha \text{ or } \theta = \pi/2\}, \quad (12)$$

which corresponds to both types of binary collisions: SBC and DBC.

260 3. Escape orbits

Notice that there are two different ways for the particles to escape to infinity.
In one case, the outer bodies escape, while the inner bodies perform consecutive
single binary collisions –escape of type 1–. In the other case, all the bodies
escape performing consecutive double binary collisions –escape of type 2–.

265 **Definition 2.** A solution of the SC4BP is an escape orbit if some or all particles go to infinity forwards or backwards in time. More concretely, it has an escape of type 1 if $y \rightarrow +\infty$ while x remains bounded, whereas it has an escape of type 2 if $x, y \rightarrow +\infty$.

Notice that when the escape is of type 1, the solution stays in the region $\theta > \theta_c$ when $s \rightarrow \pm\infty$ (forwards/backwards), so only SBC occur (collisions of type 1). Similarly, when the escape is of type 2, the solution stays in the region $\theta_\alpha < \theta < \theta_c$ when $s \rightarrow \pm\infty$ (forwards/backwards), so only DBC occur (collisions of type 2).

275 Sekiguchi and Tanikawa [12] (Theorem 5) established analytical sufficient conditions to determine when an orbit is an escape orbit. We follow the same arguments to derive the same criteria in our variables, so we do not repeat their proof here.

Proposition 1. Let $P = (r, v, \theta, w)$ be a point in the phase space \mathcal{F} , $\gamma(s)$ be a solution of the equations (6) that goes through P , and $\delta = \tan(\theta_c)$ (given in (10)).

1. For $\theta > \theta_c$, let $\Upsilon = v \sin \theta + \frac{w}{\Delta(\theta)} \cos \theta$. If

$$\sin \theta \Upsilon^2 \geq \alpha^{3/2} \sqrt{2} \left(\alpha + 8\delta^2 \frac{\delta^2 + \alpha}{(\delta^2 - \alpha)^2} \right),$$

then the orbit has an escape of type 1.

2. For $\theta < \theta_c$, let $\Upsilon = -w\sqrt{W(\theta)} + v \cos^2 \theta + v\sqrt{\alpha} \cos \theta \sin \theta$. If

$$\sec \theta (1 + \sqrt{\alpha} \tan \theta) \Upsilon^2 \geq (1 + \alpha)^2 \sqrt{2} \left(\frac{1}{(1 - \sqrt{\alpha}\varepsilon)^2} + \frac{\alpha^3}{(\sqrt{\alpha} + \varepsilon)^2} + \frac{8\alpha^2}{(2\sqrt{\alpha} + (1 - \alpha)\varepsilon)^2} \right),$$

where $\varepsilon = (\delta - \sqrt{\alpha})/(1 + \delta\sqrt{\alpha})$, then the orbit has an escape of type 2.

In both cases, the orbit escapes forwards or backwards in time depending on whether Υ is positive or negative, respectively.

285 Next, we use the above criteria and the linear approximation of the parametriza-
tion of the invariant manifolds to show that there are orbits that escape forwards
(or backwards) in time and have only one type of binary collisions. We call them
ejection-direct escape orbits of type 1 or type 2 depending on the type of the
escape. In particular, this result shows that there exists solutions of the SC4BP
290 that do not cross the section $\{\theta = \theta_c\}$ (see Section 2.3).

Theorem 1. *There exist ejection-direct escape orbits of type 1 and of type 2, that is, orbits starting (or ending) at the quadruple collision and escaping to (coming from) infinity with binary collisions only of one type.*

PROOF. By the symmetry of the problem, it is enough to prove that there exist
295 orbits on $W^u(E^+)$ that escape forwards in time performing binary collisions
only of one type. We will prove the result for orbits that have only SBC. The
proof to obtain orbits with only DBC is similar.

We will use the criteria given in Proposition 1. As we want to prove escape
forwards in time of type one, we must see that

$$\begin{aligned} F(v, \theta, w) &= \Upsilon^2 \sin \theta - \alpha^{3/2} \sqrt{2} \left(\alpha + 8\delta^2 \frac{\delta^2 + \alpha}{(\delta^2 - \alpha)^2} \right) \geq 0, \\ \Upsilon(v, \theta, w) &= v \sin \theta + w \cos \theta / \Delta(\theta) > 0. \end{aligned}$$

Using the approximation of the parametrization of order 1 of the invariant
manifold $\Psi_1^+(\xi, \varphi)$ given in (11) and (21), and omitting the variable r , a point
on $W^u(E^+)$ close to the equilibrium point can be written, for ξ small enough,
as

$$p = (v, \theta, w) = p_0 + p_1 + O(\xi^2),$$

300 where $p_0 = (v_c, \theta_c, 0)$ and p_1 are the terms of order 1 in ξ for values $\varphi \in$
 $(1/4, 1/2)$, so that we ensure that $\theta > \theta_c$ and the initial condition is in the
region of SBC.

Clearly $\Upsilon(p) = \Upsilon(p_0) + O(\xi) = v_c \sin \theta_c + O(\xi) > 0$ for ξ small enough. Next,
consider $F(p) = F(p_0) + DF(p_0) \cdot p_1 + O(\xi^2)$. On one hand, $\Upsilon(p_0)^2 \sin \theta_c =$
 $2V(\theta_c) \sin^3 \theta_c$, where $V(\theta)$ is the potential function given in (4). Using that

$V'(\theta_c) = 0$, after some computations, one can get that $F(p_0) = 0$. On the other hand,

$$DF(p_0) = 2v_c \sin^2 \theta_c \left(\sin \theta_c, \frac{3v_c}{2} \cos \theta_c, \frac{\cos \theta_c}{\Delta(\theta_c)} \right),$$

and using (21)

$$DF(p_0) \cdot p_1 = 2\xi v_c \sin^2 \theta_c \left(\frac{-h \sin \theta_c}{\sqrt{h^2 + v_c^2}} \cos(2\pi\varphi) + \frac{\cos \theta_c}{\sqrt{1 + \lambda_3^2}} \left(\frac{3v_c}{2} + \frac{\lambda_3}{\Delta(\theta_c)} \right) \sin(2\pi\varphi) \right) \quad (13)$$

where $h < 0$, $\Delta(\theta_c) > 0$ (see (5)) and $\lambda_3 = \lambda_3(E^+) > 0$. Therefore, if we consider values $\varphi = 1/4 + \varepsilon$, $DF(p_0) \cdot p_1 > 0$, which concludes the proof.

305 The proof of Theorem 1 shows that the orbits with initial conditions $\Psi_1^\pm(\xi, \varphi)$ with $\varphi = 1/4 + \varepsilon$ are the ones that escape (forwards/backwards) directly to infinity exhibiting only SBC (type 1) (analogous with $\varphi = 3/4 - \varepsilon$ and DBC). Recall that the values $\varphi = 1/4, 3/4$ correspond to the fast direction on the invariant manifold, whereas $\varphi = 1/2$ corresponds to the homothetic and the
310 slow direction. Therefore, the farther an initial condition from the homothetic solution is, the higher the probability to escape directly to infinity.

We show numerically, for $\alpha = -1$ and $h = -1$, that the orbits with initial conditions $\Psi_8^+(\xi, \varphi)$ for $\varphi = 1/4 + \varepsilon$ and $\varphi = 3/4 - \varepsilon$ are the ones that escape directly. We consider the unstable manifold $W^u(E^+)$, $\xi = 10^{-2}$ and vary $\varphi \in$
315 $(1/4, 3/4)$. Given an initial condition, we integrate the ODE (6) forwards in time and, at each step, we control the escape condition. If the condition is satisfied and the orbit has not crossed the section $\{\theta = \theta_c\}$, we save the time s_e at that point. In Figure 5 we show, on the left, that for all values of $\varphi \in (1/4, 0.49998)$ all the orbits escape directly with collisions only of type 1. A similar behavior
320 is shown for $\varphi \in (0.500006, 3/4)$ (right plot), with orbits escaping directly with collisions only of type 2. In Figure 5, some examples of direct escape are plotted for $s \leq s_e$.

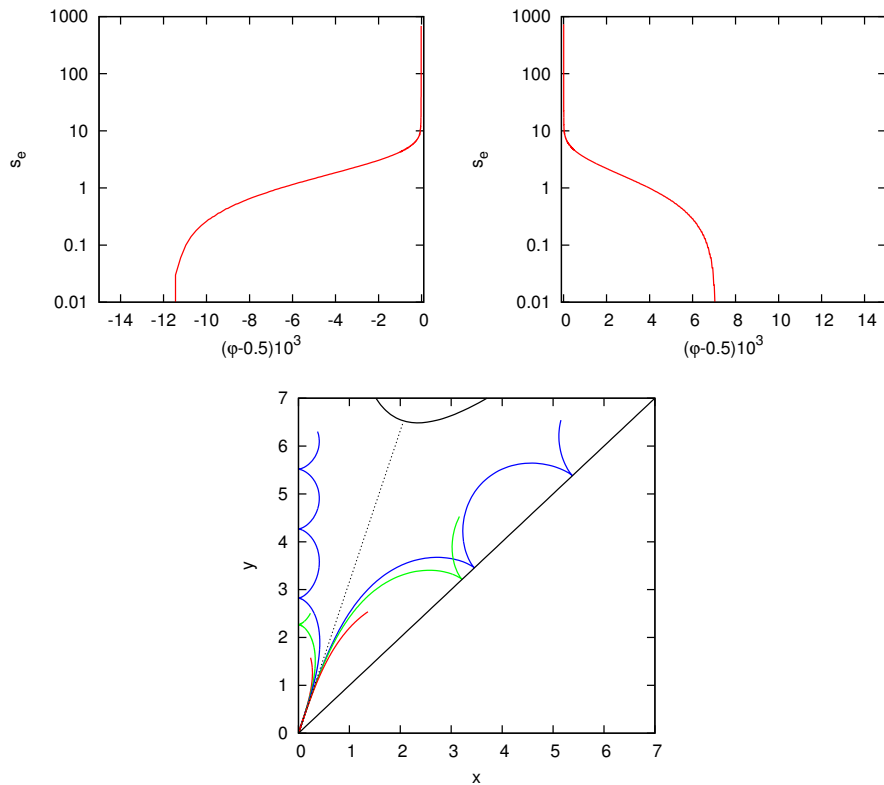


Figure 5: For orbits on $W^u(E^+)$ with initial conditions $\Psi_{\mathfrak{s}}^+(0.01, \varphi)$ for $\alpha = 1$ and $h = -1$, we plot the time s_e (in logarithmic scale) at which the escape condition through the SCB (top left plot) or DCB (top right plot) regions is satisfied without crossing $\theta = \theta_c$. Bottom: some example of orbits of direct escape, for $s \leq s_e$.

4. Ejection-collision orbits

In this Section we present some results about the ejection-collision orbits, as
 325 well as the methodology to compute and classify them. Also the results obtained
 for $\alpha = 1$ are presented.

Definition 3. *An ejection-collision orbit (ECO) of the SC4BP is a solution $\Gamma = \{\gamma(s)\}_{s \in \mathbb{R}}$ of (6) such that $\lim_{s \rightarrow \pm\infty} r(s) = 0$.*

An ECO is a solution that starts and ends in a quadruple collision. Therefore,

the orbit belongs to the intersection $W^u(E^+) \cap W^s(E^-)$. More concretely,

$$\lim_{s \rightarrow -\infty} \gamma(s) = E^+, \quad \lim_{s \rightarrow +\infty} \gamma(s) = E^-,$$

so it is a heteroclinic connection between the two equilibrium points.

330 Using the symmetry of the problem given by (8), we can prove the following statements:

Proposition 2. *Let Γ be a solution of the SC4BP.*

1. *If $\Gamma \in W^u(E^+)$ is a symmetric solution (see Definition 1), then it is an ECO.*
- 335 2. *If Γ is an ECO, then $\bar{\Gamma}$ (defined in (9)) is also an ECO.*

PROOF. By definition, if $\Gamma \in W^u(E^+)$, then $\lim_{s \rightarrow -\infty} r(s) = 0$. If the solution is symmetric, then $\lim_{s \rightarrow +\infty} r(s) = 0$, so it is an ECO.

If $\Gamma = \{\gamma(s)\}_{s \in \mathbb{R}}$ is an ECO, then it connects $E^+ \rightarrow E^-$. Then, by definition of $\bar{\gamma}(s)$

$$\lim_{s \rightarrow -\infty} \bar{\gamma}(s) = E^+, \quad \lim_{s \rightarrow +\infty} \bar{\gamma}(s) = E^-.$$

Therefore $\bar{\Gamma}$ is an ECO.

If Γ is an ECO, both Γ and $\bar{\Gamma}$ trace the same path in the configuration space (r, θ) (or (x, y)) in opposite sense.

Notice that, if a solution $\Gamma = \{\gamma(s)\}_{s \in \mathbb{R}} \in W^u(E^+)$, then $\lim_{s \rightarrow -\infty} \theta(s) = \theta_c$. Therefore, Γ only can have a finite number of binary collisions backwards in time, so there exists a *first* binary collision. Recall that the binary collisions can be viewed as the intersections of a solution with the section Σ_c . We define

$$p_j = \begin{cases} 1 & \text{the } j\text{-th intersection is a SBC,} \\ 2 & \text{the } j\text{-th intersection is a DBC,} \end{cases} \quad \text{for } j = 1, \dots, n.$$

Let B be the set of all possible sequences just taking into account the elements 1 and 2. Thus, we can define

$$\begin{aligned} P : W^u(E^+) &\longrightarrow B \\ \Gamma &\longrightarrow (p_1, p_2, \dots, p_n, \dots) \end{aligned} \tag{14}$$

Using the map P we have the following characterizations and properties.

340 **Proposition 3.** *Let $\Gamma \in W^u(E^+)$. Then*

1. $P(\Gamma)$ is finite if and only if it corresponds to an ECO.
2. If Γ is an ECO such that $P(\Gamma) = (p_1, p_2, \dots, p_n)$, then $\bar{\Gamma}$ is an ECO with $P(\bar{\Gamma}) = (p_n, p_{n-1}, \dots, p_1)$.
3. Γ is a symmetric ECO if and only if $P(\Gamma)$ is a symmetric sequence.

345 The proof of the first statement is straightforward using that both limits $\lim_{s \rightarrow \pm\infty} \theta(s) = \theta_c$, so an ECO cannot have an infinite number of binary collisions. The second one comes from the definition of a symmetric solution $\bar{\Gamma}$. The last one is clear using that $P(\Gamma) = P(\bar{\Gamma})$.

Definition 4. Γ is an ECO of order n if $P(\Gamma) = (p_1, p_2, \dots, p_n)$.

350 If an ECO of order n is symmetric, depending on the parity of n , it must touch the zero velocity curve.

Proposition 4. *Let Γ be a symmetric ECO of order n . Then, the orbit has a point on the zero velocity curve if and only if n is even. In this case, such point takes place between the $(n/2)$ -th and $(n/2 + 1)$ -th double collision.*

355 **PROOF.** If $\Gamma = \{\gamma(s)\}_{s \in \mathbb{R}}$ is symmetric, then there exists a time s_0 such that the orbit traces the same trajectory in the (r, θ) plane before and after s_0 . Therefore, $\gamma(s_0)$ is a point of return and the number and type of binary collisions must be the same before and after s_0 . Thus, n must be even and the point must be on the zero velocity curve.

360 The dynamics on the total collision manifold \mathcal{C} is the key to prove the existence of ECO. In [20], the authors use that information to show the existence of some ECO for specific values of α . In particular, they prove that for any value of the mass parameter α and for any natural number n there exists an ECO exhibiting only and exactly n SBC or n DBC. They also prove that for $\alpha \in (\alpha_3, \alpha_4)$ (see Section 2.2), an ECO with $P(\Gamma) = (1, 2, 1, 2, 1)$ exists (in particular this is true for $\alpha = 1$).

Our aim is to present a methodology to compute and classify the ECO for any fixed value of α . We will show and analyze the results obtained for the specific value $\alpha = 1$.

370 *4.1. Methodology*

In order to look for heteroclinic connections between the two equilibrium points, the main idea is to analyze the successive intersections of the orbits of the invariant manifolds $W^s(E^-)$ and $W^u(E^+)$ with the section Σ_c , defined in (12). Due to the symmetry of the problem, it is enough to deal with one of the invariant manifolds. In what follows, we consider initial conditions on $W^u(E^+)$ and the approximation of its parametrization, $\Psi_m^+(\xi, \varphi)$, for a suitable m and for a fixed value of ξ . For simplicity we denote the parametrization simply by $\Psi(\varphi)$. Then, each orbit $\gamma(s) \in W^u(E^+)$ is characterized by its initial condition given by

$$\gamma(0) = \Psi(\varphi) = (r_0, v_0, \theta_0, w_0),$$

where $\varphi \in (1/4, 3/4)$. For each φ , we integrate forward in time to compute the first n intersections of $\gamma(s)$ with Σ_c . We define the map

$$\begin{aligned} P_n : (1/4, 3/4) &\longrightarrow B \\ \varphi &\longrightarrow (p_1, p_2, \dots, p_n), \end{aligned}$$

where $P_n(\varphi) = (p_1, p_2, \dots, p_n)$ codes the first n intersections with Σ_c of the solution $\gamma(s)$ with initial condition $\Psi(\varphi)$.

375 We want to notice here that for a given φ , p_1 is the first binary collision *after* the initial condition. Depending on the the initial distance ξ considered, there could exist a binary collision before the initial condition (backwards in time, towards the quadruple collision). This is specially true for values of φ near to $1/4$ and $3/4$. As we explained in Section 3, the solutions corresponding
380 to values far from $\varphi = 1/2$ (the homothetic orbit) escape directly to infinity. So the ECO will be found for values $\varphi \in (1/2 - \varepsilon, 1/2 + \varepsilon)$, for ε small, depending on α and ξ . For example, for $\alpha = 1$ and ξ of order 10^{-2} , $\varepsilon \simeq 10^{-4}$. We will

show that for such values of φ , and for the order of the ECO computed, the first binary collision takes place far away from the equilibrium point, so $P_n(\varphi)$ starts with the very first binary collision of the orbit.

Up to now, we have characterized the ejection-collisions orbits in terms of the map P . In order to detect and compute them we use the following result:

Proposition 5. *Let φ_1 and φ_2 be such that*

$$\begin{aligned} P_{n+1}(\varphi_1) &= (p_1, p_2, \dots, p_n, p_{n+1}^1), \\ P_{n+1}(\varphi_2) &= (p_1, p_2, \dots, p_n, p_{n+1}^2), \end{aligned}$$

with $p_{n+1}^1 \neq p_{n+1}^2$. Then, there exists a value $\varphi \in (\varphi_1, \varphi_2)$ such that $P(\varphi) = (p_1, p_2, \dots, p_n)$.

The proof is straightforward by continuity with respect to the initial condition φ .

Using Proposition 5, to detect the existence of an ECO of order n , we vary $\varphi \in (1/4, 3/4)$ and we compute $P_{n+1}(\varphi)$ integrating the equations (6) of the SC4BP up to the $(n+1)$ -th crossing with Σ_c . To detect a change in the type of the binary collision, it is enough to track the value of θ at the $(n+1)$ -th crossing, $\theta_{n+1}(\varphi)$: when it changes from $\pi/2$ to θ_α , or the other way around, we are in the situation of Proposition 5. Although the discontinuities of the function $\theta_{n+1}(\varphi)$ show the existence of ECO, we propose to use, instead, the function $F_{n+1}(\varphi) = r(\theta - \theta_c)$, where r and θ are the values of the orbit at the $(n+1)$ -th intersection with the section Σ_c (or the $(n+1)$ -th binary collision). Clearly, the function F_{n+1} is continuous and due to the fact that $r > 0$, it changes sign depending on whether θ is greater or smaller than θ_c . Therefore, each solution of $F_{n+1}(\varphi) = 0$ corresponds to an ECO orbit of order $j \leq n$. We track the sign of the function F_{n+1} and apply an iterative method to obtain the value of φ (up to a certain precision) that corresponds to the ECO. We have repeated the explorations for $\alpha = 1$ and different values of $\xi = 0.001, 0.01, 0.05$. In all cases we have obtained the same results (that is, the same ECO). In Figure 6 we show the values of $\theta_n(\varphi)$ and $F_n(\varphi)$ for $n = 5, 6, 7$ and $\varphi < 1/2$,

410 using $\alpha = 1$ and $\xi = 0.05$ and $h = -1$. For $n = 5$ the function F_5 shows four zeros, corresponding to four ECO of order $n \leq 4$ (see Table 1 in next Section), for $n = 6$, the function F_6 shows six zeros, corresponding to the same ECO and two new ones, of order 5. And so on.

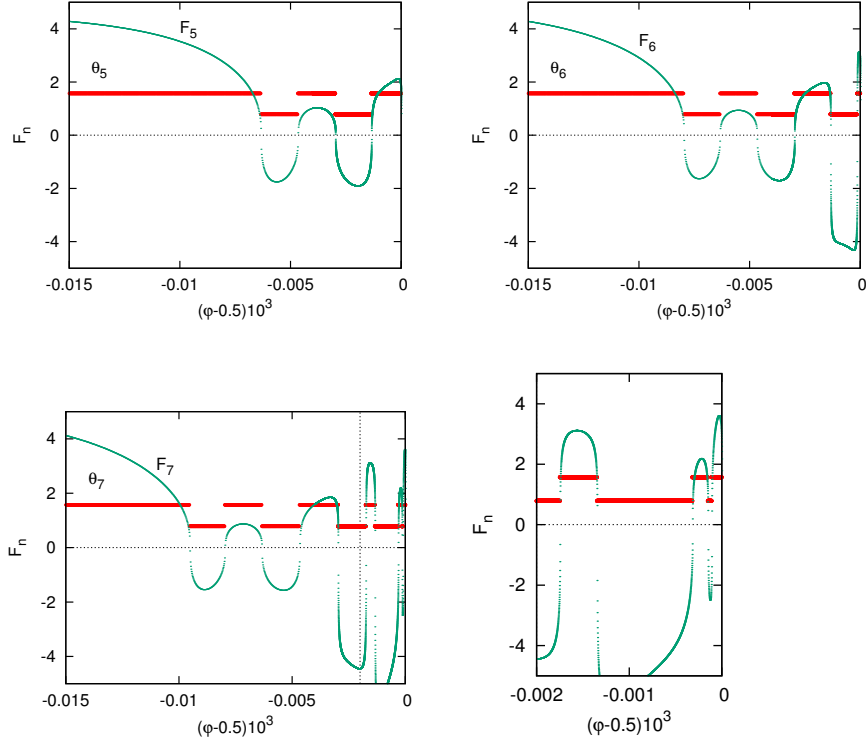


Figure 6: Functions $\theta_n(\varphi)$ and $F_n(\varphi) = r(\theta - \theta_c)$ for $\alpha = 1$, $h = -1$, $\varphi < 1/2$ and $n = 5, 6$ (first row) and $n = 7$ (second row; on the right, the plot shows a detail showing five of the zeros of the function). $\alpha = 1$, $h = -1$.

We want to notice two important issues. On one hand, the bigger the order
 415 n , the smaller the interval $I = (1/2 - \varepsilon, 1/2 + \varepsilon)$ where some of the zeros of F_n
 exist. But, fixed an order n , the bigger the value of ξ , the larger the interval I
 that must be taken. Therefore, in order to look for the zeros of F_n with a good
 accuracy, it is important to start with the bigger ξ admissible, so a high order
 approximation of the parametrization of the invariant manifold is needed.

On the other hand, up to the values of n computed, we find that all of the zeros of the functions F_n are transversal. If this observation was true for any ECO, the result of the Proposition 5 would be an *if and only if* result. That is, if the ECO of order n corresponds to $\bar{\varphi}$ and

$$P(\bar{\varphi}) = (\bar{p}_1, \dots, \bar{p}_n)$$

420 then

$$\begin{aligned} P_{n+1}(\bar{\varphi} + \epsilon) &= (\bar{p}_1, \dots, \bar{p}_n, p_{n+1}^1) \\ P_{n+1}(\bar{\varphi} - \epsilon) &= (\bar{p}_1, \dots, \bar{p}_n, p_{n+1}^2) \end{aligned}$$

where $p_{n+1}^1 \neq p_{n+1}^2$ for ϵ small enough. Numerically we observe that this is true.

4.2. Results

We present here, for $\alpha = 1$ and $h = -1$, the ECO computed up to order $n \leq 7$ by looking for the zeros of the function $F_8(\varphi)$ as explained in the previous
425 Section. The orbits obtained are summarized in Tables 1– 4. Recall that, for any ECO of order n of type (p_1, \dots, p_n) , there exists also the symmetric one (p_n, \dots, p_1) that traces the same path in configuration space, so they are not included.

For $n \leq 4$, only ECO of type $(1, \dots, 1)$ or $(2, \dots, 2)$ exist, so there are only
430 two ECOs for each order, see Table 1. For $n = 5$ we find four different ECO, all of them symmetric, see Table 2. The first non-symmetric orbits are found for $n \geq 6$. For $n = 6$, there exist eight different ECOs, two symmetric and six non-symmetric, see Table 3. We plot three of the non-symmetric ones, the other three are obtained by symmetry, and have the same projection in the
435 configuration space. Similarly, for $n = 7$, there exists twelve different ECOs, four of them symmetric, see Table 4.

Notice that, as was stated in Proposition 4, when n is even, the symmetric orbits have a point on the zero velocity curve.

In [20], Lacombe and Medina give a graph, for certain values of α , that allows
440 to identify the possible sequences of binary collisions for an orbit passing near

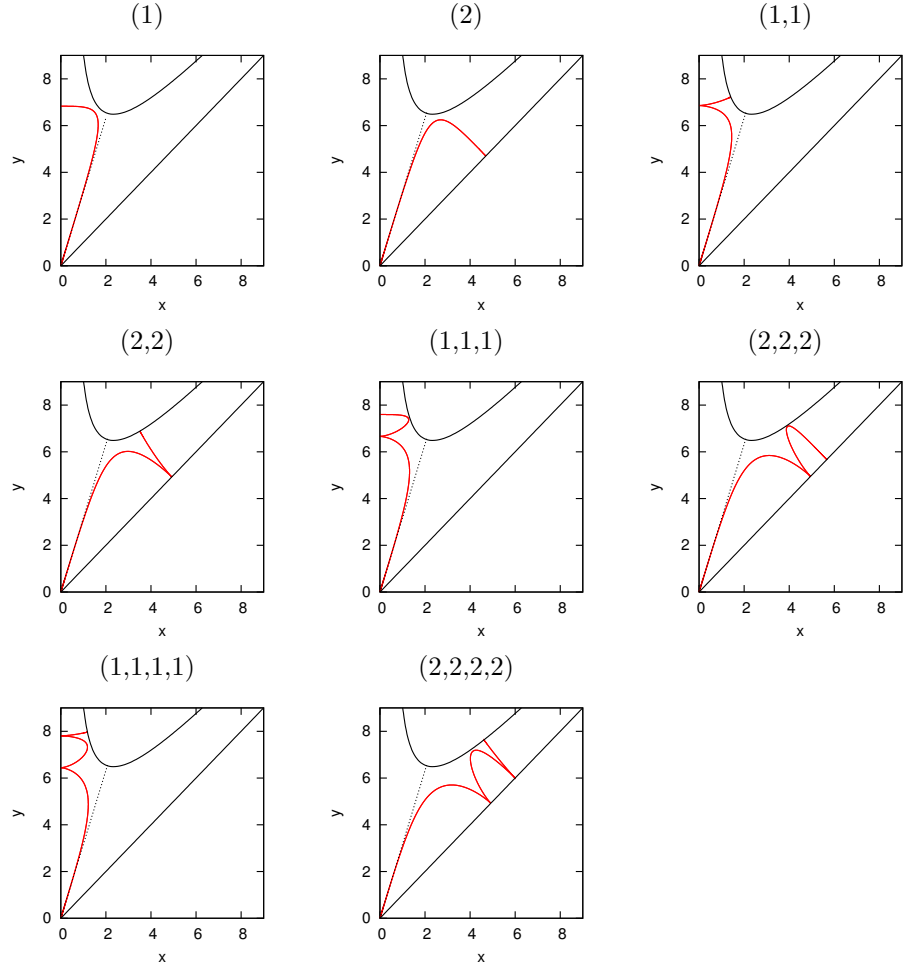


Table 1: For each order $n = 1, \dots, 4$ only two ECOs are found, all of them exhibiting binary collisions of only one type for $\alpha = 1$ and $h = -1$.

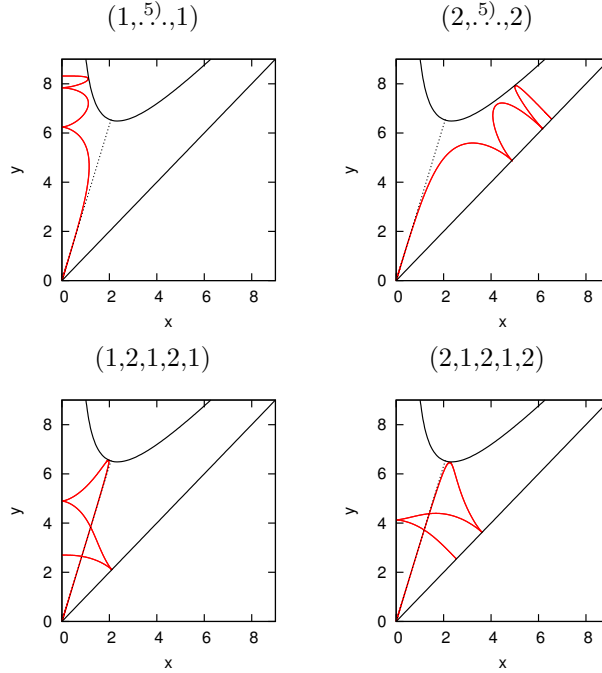


Table 2: ECOs obtained for $n = 5$ with $\alpha = 1$ and $h = -1$. All of them are symmetric.

the total collision. We reproduce (in our notation) that graph in Figure 7 for $\alpha = 1$. As was noticed also in [12], not all the possible sequences are realizable. In particular, not all of the sequences in the graph of Lacomba and Medina are satisfied, but it provides the sequences of binary collision that are not admissible
445 for orbits close to quadruple collision. For example, from the graph in Figure 7 it is clear, that no ECO orbits of types $(2, \cdot^k), 2, 1, 1)$ and $(1, \cdot^k), 1, 2, 2)$ can exist.

5. Discussion and conclusions

As stated in [12], the invariant manifolds $W^{s,u}(E^\pm)$ separate different kinds of dynamical behaviors taking into account the type of binary collisions. In
450 particular, their intersections correspond to the ejection-collision orbits from/to quadruple collision. On one hand, we present here a specific characterization of the ECO and a methodology to compute them for any value of the mass

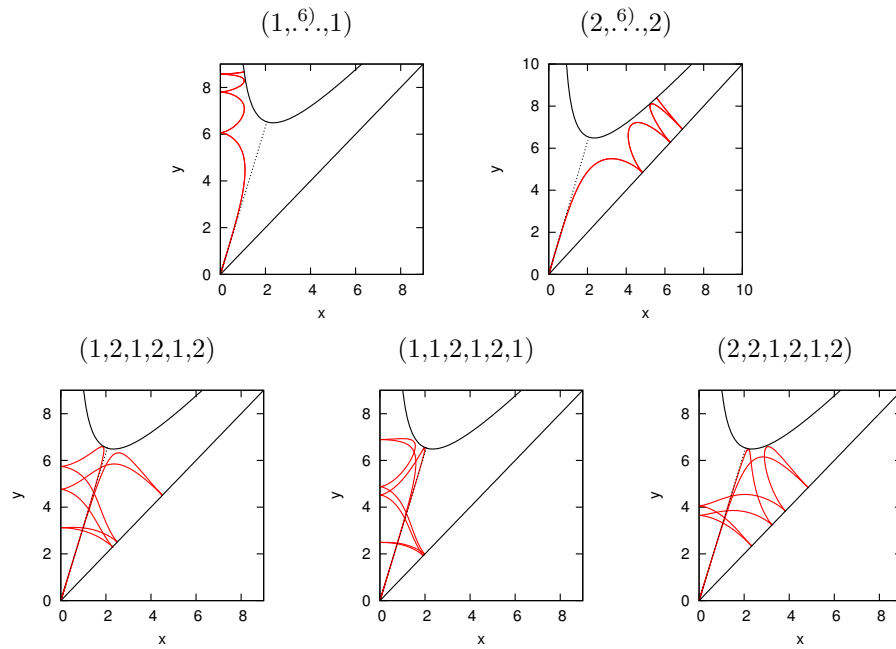


Table 3: ECOs obtained for $n = 6$ with $\alpha = 1$ and $h = -1$. First row, symmetric orbits. Second row, non-symmetric orbits. Their symmetric ones, which have the same projection on the (x, y) plane, are the ECOs $(2, 1, 2, 1, 2, 1)$, $(1, 2, 1, 2, 1, 1)$ and $(2, 1, 2, 1, 2, 2)$.

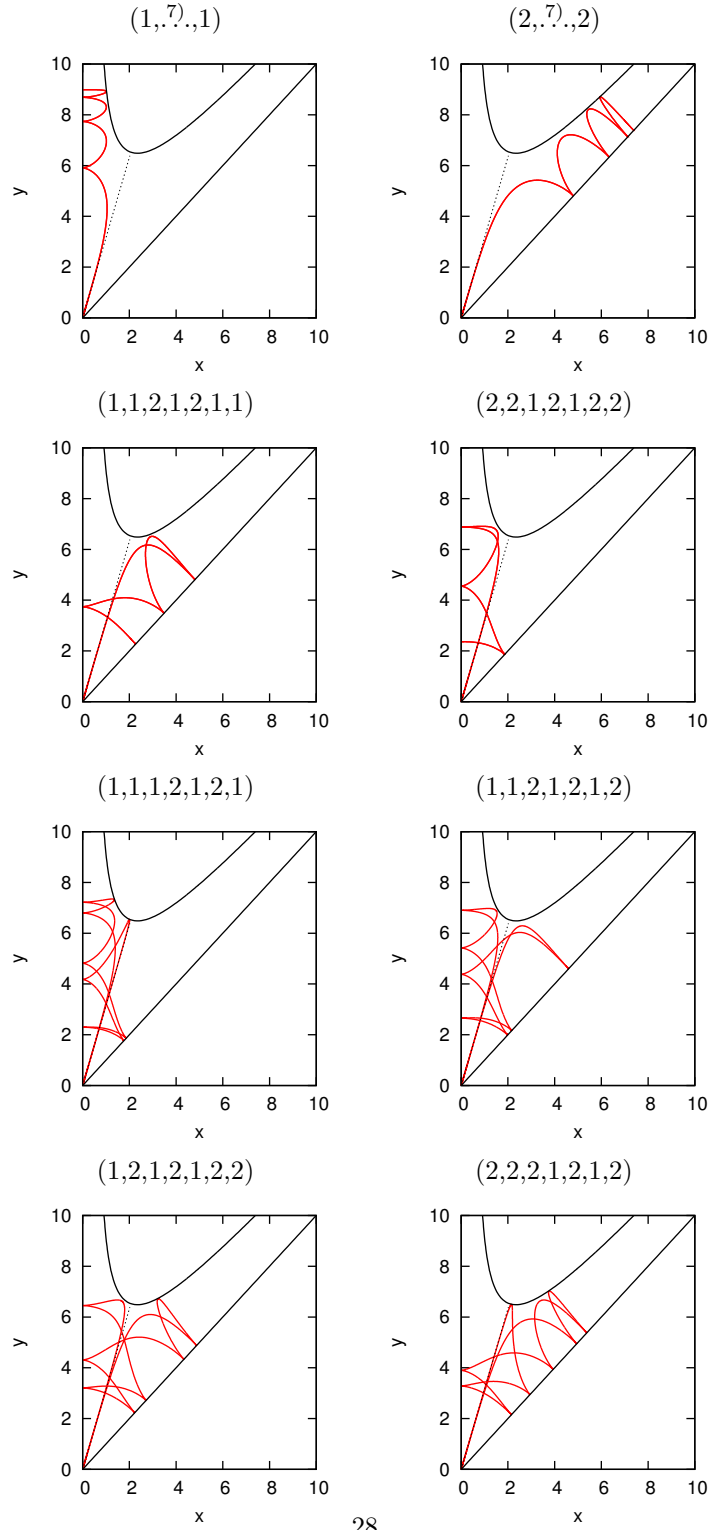


Table 4: ECOs for $n=7$ with $\alpha=1$ and $h=-1$. Symmetric ones (first and second rows). Non symmetric ones (third and fourth rows). Their symmetric ones, which have the same projection on the (x, y) plane, are the ECOs $(1,2,1,2,1,1,1)$, $(2,1,2,1,2,1,1)$, $(2,2,1,2,1,2,1)$ and $(2,1,2,1,2,2,2)$.

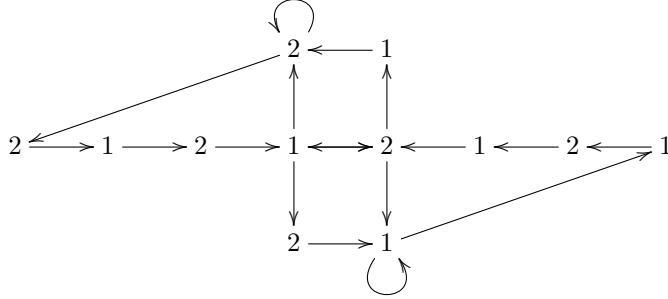


Figure 7: Graph for admissible sequences of binary collisions for orbits passing near the total collision for $\alpha = 1$.

parameter α and negative energy h . The method presented uses as a Poincaré section Σ_c that corresponds to the binary collisions DBC and SBC. The difference with the mentioned work is that they use as a Poincaré section the plane that contain the homothetic $\{\theta = \theta_c\}$, which is not suitable for the computation of the ECOs. The methodology also relies in the computation of an approximation of order m (for a suitable m) of the parametrization of the invariant manifolds. On the other hand, the approximated parametrization allows us to prove that there exist orbits that eject from quadruple collision and escape to infinity performing only binary collisions of one type (direct escape). Clearly, the same is true reversing time (orbits ending in quadruple collision). Our guess is that there should be a separation between those ejection orbits that escape directly with one type of binary collisions and the remaining ejection-escape orbits (with several mixed types of binary collisions). Of course, this separation should be visible by computing the connections between the invariant manifolds of E^+ and E^- and the manifolds of the infinity. But this is work for a future paper.

Although the methodology described applies for any value of $\alpha > 0$, $h < 0$ and any given order n for the ECO, we present the results obtained for $\alpha = 1$ and $h = -1$, and show ECO up to order $n = 7$. We also remark that different results, concerning the type of ECO, may be expected depending on α . More precisely, for $\alpha = 1$, we notice that if there exists an ECO of type (p_1, \dots, p_n) , then we also find the ECO of type $(\hat{p}_1, \dots, \hat{p}_n)$, with $\hat{p}_j = 3 - p_j$. This seems to be related with the same topological behaviour, concerning SBC and DBC,

of the invariant manifolds of E^\pm on the quadruple collision manifold (but no analytical proof is known so far). However, as shown in Figure 3 for $\alpha = 2$, the behaviour of such manifolds, and therefore the type of ECO obtained, varies with α .

480 6. Appendix

Here we present in detail some results concerning the eigenvalues and eigenvectors associated to the equilibrium points for any values of α and $h < 0$. We give their expressions in terms of h , v_c and θ_c , and the explicit formulae for the approximations of the invariant manifolds of order one $\Psi_1^\pm(\xi, \phi)$.

Recall that the equilibrium points are $E^\pm = (0, \pm v_c, \theta_c, 0)$, where θ_c is the minimum of V (defined in (4)) and $v_c^2 = V(\theta_c)$. Then, $V'(\theta_c) = 0$ and $V''(\theta_c) > 0$. The eigenvalues associated to the equilibrium points are

$$\begin{aligned} \lambda_1(E^\pm) &= \pm\lambda, & \lambda_2(E^\pm) &= -\lambda_1, \\ \lambda_3(E^\pm) &= \frac{\lambda}{4} \left(\mp 1 + \sqrt{1 + \frac{8V''(\theta_c)}{V(\theta_c)}} \right), & \lambda_4(E^\pm) &= \frac{\lambda}{4} \left(\mp 1 - \sqrt{1 + \frac{8V''(\theta_c)}{V(\theta_c)}} \right), \end{aligned} \quad (15)$$

485 where $\lambda = \sqrt{2 \cos \theta_c (\sin \theta_c - \sqrt{\alpha} \cos \theta_c)} > 0$. Notice that $\lambda_3 > 0$ and $\lambda_4 < 0$, and $\lambda_3 \neq \lambda_4$. Next we prove that all the eigenvalues are different for any value of α .

Lemma 1. *Let $\lambda_i(E^\pm)$, $i = 1, \dots, 4$, be the eigenvalues associated to the equilibrium points E^\pm of the SC4BP. Then, for all values of α :*

- 490
1. all the eigenvalues are different: $\lambda_i \neq \lambda_j$, $i \neq j$,
 2. $0 < \lambda_1(E^+) < \lambda_3(E^+)$, and $0 > \lambda_1(E^-) > \lambda_4(E^-)$.

PROOF. Notice that, from (15), the two inequalities of the second statement are equivalent, so it is enough to prove one of them. Moreover, it is not difficult to see that both statements are equivalent to see

$$V''(\theta_c) - 3V(\theta_c) > 0 \quad \text{and} \quad V''(\theta_c) - V(\theta_c) \neq 0, \quad (16)$$

where θ_c is the unique solution of $V'(\theta) = 0$, and V is given in (4). We write

$$V(\theta) = \frac{\sqrt{2}}{2 \cos \theta} h(z) \text{ where } z = \tan \theta > \sqrt{\alpha} \text{ and}$$

$$h(z) = 1 + \frac{\alpha^{5/2}}{z} + 8\alpha^{3/2} \frac{z}{z^2 - \alpha}.$$

Then

$$\begin{aligned} V'(\theta) &= \frac{\sqrt{2}}{2 \cos \theta} (zh(z) + h'(z)(z^2 + 1)), \\ V''(\theta) &= \frac{\sqrt{2}}{2 \cos \theta} (z(zh(z) + h'(z)(z^2 + 1)) \\ &\quad + (h(z) + 3zh'(z) + (z^2 + 1)h''(z))(z^2 + 1)), \end{aligned}$$

where the prime ' denotes derivative with respect z .

The condition $V'(\theta_c) = 0$ is equivalent to

$$z_c h(z_c) + h'(z_c)(z_c^2 + 1) = 0, \quad (17)$$

where $z_c = \tan(\theta_c)$. Introducing this relation into the expression for $V''(\theta_c)$, we have that the conditions in (16) write

$$V''(\theta_c) - 3V(\theta_c) = \frac{\sqrt{2}}{2 \cos \theta_c} (1 + z_c^2) ((1 + z_c^2)h''(z_c) - 2h(z_c)) > 0 \quad (18)$$

and

$$V''(\theta_c) - V(\theta_c) = \frac{\sqrt{2}}{2 \cos \theta_c} ((1 + z_c^2)^2 h''(z_c) - 2z_c^2 h(z_c)) \neq 0, \quad (19)$$

where z_c is the solution of (17).

We introduce the change $z_c = \sqrt{\alpha} w$ in (17), where $w > 1$. Simplifying, the equation transforms into

$$w^7 - 2w^5 - (8 + 17\alpha)w^4 + w^3 + (2\alpha - 8)w^2 - \alpha = 0.$$

The equation is lineal in α , and $17w^4 - 2w^2 + 1 > 0$ for $w > 1$. Therefore, we can write

$$\alpha = \frac{w^2(w^5 - 2w^3 - 8w^2 + w - 8)}{17w^4 - 2w^2 + 1}. \quad (20)$$

⁴⁹⁵ Imposing the condition $\alpha > 0$, we have that $w > \bar{w}$, where $\bar{w} \in [11/5, 12/5]$ is the only positive root of $w^5 - 2w^3 - 8w^2 + w - 8 = 0$.

We introduce the change $z_c = \sqrt{\alpha} w$ in (18) and (19), and simplifying and keeping the numerators, we get that both conditions are equivalent, respectively, to

$$w^9 - 3w^7 - (41\alpha + 8)w^6 + 3w^5 + (11\alpha - 24)w^4 - w^3 - 3\alpha w^2 + \alpha > 0$$

and

$$\begin{aligned} \alpha w^{11} - 3\alpha w^9 - (42\alpha^2 + 16\alpha)w^8 + 3\alpha w^7 + (14\alpha^2 - 49\alpha - 8)w^6 \\ - \alpha w^5 - (6\alpha^2 - 3\alpha + 24)w^4 + (2\alpha^2 - 3\alpha)w^2 + \alpha \neq 0. \end{aligned}$$

Finally, we introduce (20) in the above expressions, and they are equivalent to

$$\begin{aligned} (w - 1)(w + 1)(3w^2 + 1)(w^7 - w^5 - 8w^4 + w^2 - 1) > 0 \\ (w - 1)^5(w + 1)^3(w^7 - w^5 - 8w^4 + w^2 - 1) \\ \times (25w^5 + 50w^4 + 80w^3 + 46w^2 + 15w + 8) \neq 0 \end{aligned}$$

for $w > \bar{w}$. The computation of the zeros of the term $w^7 - w^5 - 8w^4 + w^2 - 1$ gives that it is positive for $w > 11/5$, so both statements are true.

The first result of Lemma 1 implies that for all values of α there exist 2-
500 dimensional invariant manifolds $W^u(E^+)$ and $W^s(E^-)$. The tangent space to the unstable manifold $W^u(E^+)$ is generated by the eigenvectors associated to λ_1 and λ_3 . The tangent space to the stable manifold $W^s(E^-)$ is generated by the eigenvectors associated to λ_1 and λ_4 . The corresponding eigenvectors $\sigma_i(E^\pm)$ can also be written in terms of θ_c , v_c and the energy as

$$\begin{aligned} \sigma_1(E^\pm) &= (-v_c, \mp h, 0, 0), \\ \sigma_3(E^\pm) &= (0, 0, 1, \lambda_3), \\ \sigma_4(E^\pm) &= (0, 0, 1, \lambda_4). \end{aligned}$$

505 Therefore, we can write the approximations of order one of the parametrizations of the invariant manifolds. For example, using the normalized eigenvectors

$\bar{\sigma}_i = \sigma_i / \|\sigma_i\|$, we have that for $W^u(E^+)$:

$$\begin{aligned} \Psi_1^+(\xi, \phi) &= E^+ + \xi (\cos(2\pi\varphi) \bar{\sigma}_1 + \sin(2\pi\varphi) \bar{\sigma}_3) \\ &= \begin{pmatrix} 0 \\ v_c \\ \theta_c \\ 0 \end{pmatrix} + \xi \begin{pmatrix} \frac{-v_c}{\sqrt{h^2 + v_c^2}} \cos(2\pi\varphi) \\ \frac{-h}{\sqrt{h^2 + v_c^2}} \cos(2\pi\varphi) \\ 1 \\ \frac{\lambda_3}{\sqrt{1 + \lambda_3^2}} \sin(2\pi\varphi) \\ \frac{\lambda_3}{\sqrt{1 + \lambda_3^2}} \sin(2\pi\varphi) \end{pmatrix}. \end{aligned} \quad (21)$$

From the second statement of Lemma 1 we have that the eigenvector associated to λ_1 gives the slow direction in both invariant manifolds, whereas the strong directions are given by the eigenvectors associated to λ_3 (for $W^u(E^+)$) and λ_4 (for $W^s(E^-)$).

As we noticed in Section 2.2, in order to have $r > 0$, we need $\cos(2\pi\varphi) < 0$, so we consider $\varphi \in (1/4, 3/4)$. The values $\varphi = 1/4, 3/4$ give the solutions along the direction σ_3 or σ_4 (the fast direction). In this case, $r = 0$ and we obtain orbits inside the collision manifold. The value $\varphi = 1/2$ gives the solution along the direction σ_1 (the slow direction), which corresponds to the homothetic solution. Notice that we could have taken $\sigma_1(E^\pm) = (v_c, \pm h, 0, 0)$. In this case, we must consider $\varphi \in (-1/4, 1/4)$, and the fast and slow directions would correspond to $\varphi = \pm 1/4$ and $\varphi = 0$, respectively.

Acknowledgements

E. Barrabés has been supported by grants MTM2016-80117-P (MINECO/FEDER, UE), and Catalan (AGAUR) grant 2017 SGR 1374. M. Ollé is partially supported by Spanish MNECO/FEDER grant MTM2015-65715 and the Catalan grant 2017SGR1049.

References

- [1] E. Lacombe, Mouvements voisins de collision quadruple dans le problème trapezoidal des 4 corps, *Celest. Mech. Dyn. Astron.* 31 (1983) 23–41.

- [2] C. Simó, E. Lacomba, Analysis of some degenerate quadruple collisions, *Celest. Mech.* 28 (1-2) (1982) 49–62.
530 URL <https://doi.org/10.1007/BF01230659>
- [3] S. Mikkola, Encounters of binaries – i. equal energies, *Mon. Not. R. Astron. Soc.* 203 (1983) 1107–1121.
- [4] S. Mikkola, Encounters of binaries -ii unequal energies, *Mon. Not. R. Astron. Soc.* 207 (1984) 115–126.
- 535 [5] S. Mikkola, Numerical simulations of encounters of hard binaries, in: *Dynamics of Star Clusters*, Proceedings of the Symposium, IAU Symposium, Symposium sponsored by IAU (1985), Vol. 113 of International Astronomical Union Symposia, Reidel, Dordrecht, 1985, pp. 335–338.
- [6] S. Mikkola, Numerical treatment of small stellar systems with binaries,
540 *Celest. Mech. Dyn. Astron.* 68 (1997) 87–104.
- [7] P. Leonard, Stellar collisions in globular clusters and the blue straggler problem, *Astron. J.* 98 (1989) 217–226.
- [8] J. Fregeau, P. Cheung, S. Portegies Zwart, F. Rasio, Stellar collisions during binary–binary and binary–single star interactions, *Mon. Not. R. Astron. Soc.* 352 (2004) 1–19.
545
- [9] M. Álvarez-Ramírez, M. Medina, A model for binary-binary close encounters and collisions from a dynamical point of view, *Astrophys. Space Sci.* 349 (2014) 143–150.
- [10] R. McGehee, Triple collision in the collinear three-body problem, *Invent. Math.* 27 (1974) 191–227.
550 URL <https://doi.org/10.1007/BF01390175>
- [11] W. Sweatman, The symmetrical one-dimensional Newtonian four-body problem: a numerical investigation, *Celest. Mech. Dyn. Astron.* 82 (2)

(2002) 179–201, the restless universe (Blair Atholl, 2000).

555 URL <https://doi.org/10.1023/A:1014599918133>

[12] M. Sekiguchi, K. Tanikawa, On the symmetric collinear four-body problem, *Publ. Astron. Soc. Jpn.* 56 (2004) 235–251.

[13] T. Ouyang, D. Yan, Periodic solutions with alternating singularities in the collinear four-body problem, *Celest. Mech. Dyn. Astron.* 109 (2011) 229–
560 239.

[14] H.-Y. Huang, Schubart-like orbits in the newtonian collinear four-body problem, *DCDS, A* 32 (2012) 1763–1774.

[15] L. Bakker, T. Ouyang, S. Simmons, D. Yan, G. Roberts, Linear stability for some symmetric periodic simultaneous binary collision orbits in the
565 four-body problem, *Celest. Mech. Dyn. Astron.* 108 (2010) 147–164.

[16] W. Sweatman, A family of symmetrical Schubart-like interplay orbits and their stability in the one-dimensional four-body problem, *Celest. Mech. Dyn. Astron.* 94 (1) (2006) 37–65.

URL <https://doi.org/10.1007/s10569-005-2289-8>

570 [17] M. Álvarez-Ramírez, M. Medina, C. Vidal, The trapezoidal collinear four-body problem., *Astrophys. Space Sci.* 358 (2015) 1–17.

[18] J. Mather, R. McGehee, *Dynamical Systems, Theory and Applications*, Vol. 38 of *Lecture Notes in Physics*, Springer, Berlin, Heidelberg, 1975, Ch. Solutions of the collinear four body problem which become unbounded in
575 finite time., pp. 573–597.

[19] A. Haro, M. Canadell, J. Figueras, A. Luque, J. Mondelo, The parameterization method for invariant manifolds. From Rigorous Results to Effective Computations., Vol. 195 of *Applied Mathematical Science*, Springer-Verlag, 2016.

- 580 [20] E. Lacomba, M. Medina, Symbolic dynamics in the symmetric collinear
four-body problem, *Qual. Theory Dyn. Syst.* 5 (1) (2004) 75–100.
URL <https://doi.org/10.1007/BF02968131>
- [21] D. Saari, Collisions, rings, and other Newtonian N -body problems, Vol.
104 of CBMS Regional Conference Series in Mathematics, Published for
585 the Conference Board of the Mathematical Sciences, Washington, DC; by
the American Mathematical Society, Providence, RI, 2005.
URL <https://doi.org/10.1090/cbms/104>
- [22] E. Lacomba, Infinity manifolds for positive energy in celestial mechanics, in:
The Lefschetz centennial conference, Part III (Mexico City, 1984), Vol. 58
590 of *Contemp. Math.*, Amer. Math. Soc., Providence, RI, 1987, pp. 193–201.